16[th] World Conference on Earthquake, 16WCEE 2017

Santiago Chile, January 9th to 13th 2017

Paper N° 1261 (Abstract ID)

Registration Code: S-R1462934770

STUDY ON THE DAMAGE DUE TO SLOSHING OF LIQUEFIED GROUND IN CHIBA CITY DURING THE GREAT EAST JAPAN EARTHQUAKE

S. Yasuda[(1)] , K. Ishikawa[(2)] , M. Urano[(3)]

[(1)] *Professor, Tokyo Denki University, yasuda@g.dendai.ac.jp*
[(2)] *Assistant Professor, Tokyo Denki University, ishikawa@g.dendai.ac.jp*
[(3)] *Graduate Student, Tokyo Denki University, 15rmg03@ms.dendai.ac.jp*

Abstract

The Great East Japan Earthquake on March 11, 2011 caused severe damage, particularly to the strip of land along the Pacific Ocean from the Tohoku Region to the Kanto Region. In the Tokyo Bay Area, widespread liquefaction destroyed a large number of wooden houses, pushed up road pavements, and damaged water and gas pipes and manholes. The liquefied ground shook repeatedly and the duration of shaking was long—the Great East Japan Earthquake lasted 3–4 minutes. After the earthquake, a field survey was conducted, targeting the liquefied areas at landfill land with low soil strength such as the landfill of the Tokyo Bay area to correlate ground motion intensity and damage severity. Liquefaction at the bottom layers occurred in inclined or irregular ground surfaces and buckling are common near this boundary. To investigate the mechanism of sloshing, two-dimensional seismic response analysis was conducted for areas where damage has occurred in Chiba using FLUSH, a two-dimensional FEM analysis. The shear modulus was reduced to 1/50, 1/100, and 1/200 of typical values. Consequently, the large compressive and tensile strains in the horizontal direction at shallow depth near the road buckling were reproduced at low *G* values, i.e., 1/100 and 1/200 of typical values. Large compressive and horizontal strain were observed near the boundaries of areas that were not affected by liquefaction within the liquefaction-affected area. Because of the long duration of ground shaking, the nonliquefied and liquefied layers repeatedly collide; consequently, large strains in the horizontal direction occurred.

Keywords: Great East Japan Earthquake, Liquefaction, Seismic response analysis

1. Introduction

The Great East Japan Earthquake of March 11, 2011 caused severe damage over a wide range of the Tohoku region and not just in the Kanto region. In particular, in the Tokyo Bay area, repeated shaking of the liquefied ground caused significant damage, e.g., the road surfaces underwent buckling damage and the joints of water pipes and gas conduits were deviated. Because the earthquake duration was long and its scale was extremely high- in magnitude, it is inferred that sloshing occurred after soil liquefied as the ground was greatly shaken.This sloshing damage was confirmed in the reclamation area that liquefied by the wide range of the Tokyo Bay area. Sloshing is classified into two patterns based on the place and topography of damage. The first pattern is “irregular ground,” in which the bottom of the liquefied layer is inclined, as shown in Figure 1. The second pattern is “ground boundaries exist,” in which a building or highway exists at the ground surface, as shown in Figure 2. In Chiba City, buckling damage of the road surfaces has frequently occurred due to sloshing, as shown in Photo.1, and has caused damage, thus presenting a major obstacle to everyday life.

We made a study in the following order to the determine the cause of the buckling damage to road surfaces that occurred from the sloshing after liquefaction in Mihama-ku Chiba City during the Great East Japan Earthquake:

1) Organize the buckling damage occurrence points on the roads in Chiba City.

2) Create a two-dimensional cross-section and calculate the initial stress in the ground.

3) Conduct a seismic response analysis to calculate the in-ground strain, displacement, and acceleration at the time of the earthquake.

The analysis programs used here are as follows:

・Initial stress analysis: Two-dimensional FEM static stress analysis ALID/Win Ver. 5.0

・Seismic response analysis: Two-dimensional FEM dynamic response analysis ADVANF/Win Ver4.0

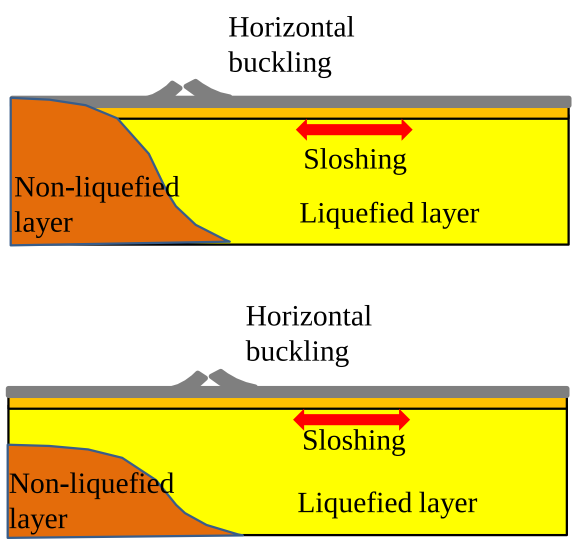

Fig.1 – Irregular ground

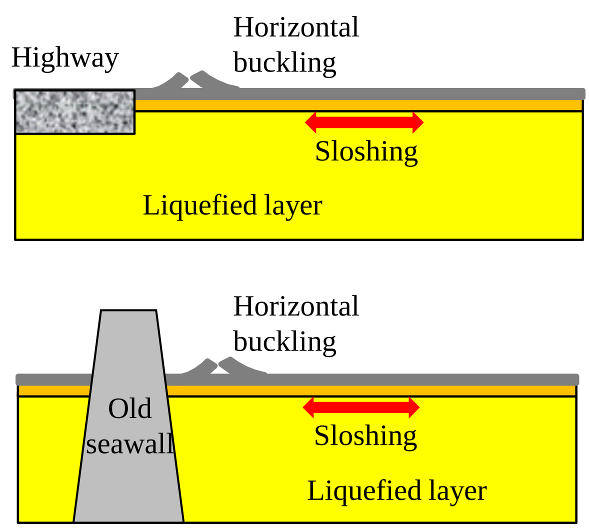

Fig.2 – Ground boundaries exist

Photo1 – Buckling damage to the road due to sloshing after liquefaction
(Chiba City, Chiba Prefecture)

2. Organization of damage points in Chiba City from the Great East Japan Earthquake

As mentioned above, the landfill of the Tokyo Bay area has received severe damage from liquefaction caused by the Great East Japan Earthquake. A field survey was performed in these areas from the day after the earthquake to map the buckling damage points on the roads (Photo.1). Figure 3 shows the buckling damage points on the roads in Mihama-ku Chiba City. This was created on the basis of the data received for Chiba City and from the results of the field survey. From this figure, we can see that buckling damage to the roads occurred at about 20 locations.

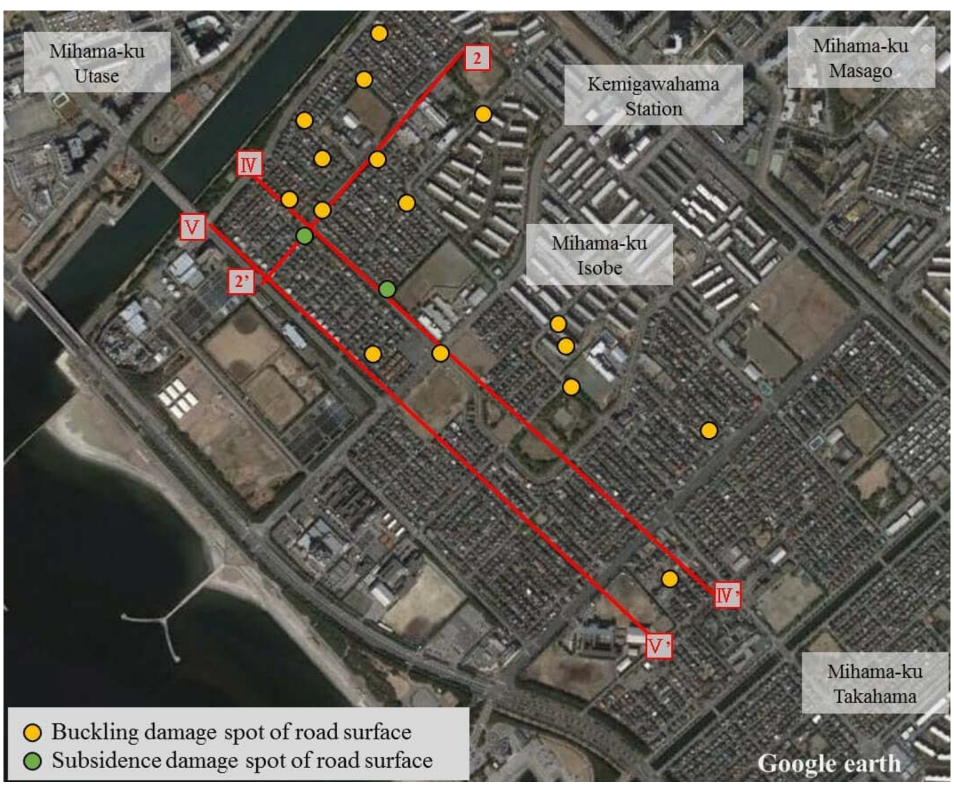

Fig.3 – Survey line positions that were used for the analysis and damage points in Mihama-ku, Chiba City

3. Study of the buckling damage to roads from sloshing using the analysis

3.1 Ground used in the analysis

The ground model used a 2–2' survey line, IV–IV' survey line, and V–V' survey line across the north–south and east–west directions in Mihama-ku, Chiba City, as shown in Figure 3. These survey lines are estimated cross-sections created by the Chiba City (2014). We created our ground models based on them. Each of the ground model diagrams is described together with an analysis of the results.

3.2 Terms and conditions of the analysis

This analysis was carried out using two methods of seismic response analysis. The first method assumed that the landfill land layer did not liquefy (Case 1). The second method assumed the occurrence of sloshing after liquefaction. In this latter case, Layer B and the Fsc layer of sandy soil landfill were assumed to have liquefied below the groundwater level. The groundwater level was used as the estimated value and was based on the boring data for various location layer cross-sections from Chiba City (2014) documents. The deformation properties of the landfill soil layer under the groundwater level were assumed to be impaired by continued shaking from liquefaction. The rates were set to 1/50 (Case 2), 1/100 (case 3), and 1/200 (Case 4), and the model used a linear method. The damping ratio was set to 20 %, and it was assumed to be constant and independent of the strain. In addition, in this earthquake, it was confirmed that the liquefied ground was shaking for a period of approximately 4 s. Considering the relationship $T = 4H/V_S$ and a liquefied layer of 8 m this liquefied ground, V_S was determined to be 8 m/s. From this value of V_S and the equation $G_0 = \rho V_S^2$, the shear modulus G_0 was determined to be approximately 100 kN/m^2. Therefore, we also performed an analysis (Case 5) in which the constant G_0 was set at 100 kN/m^2. Moreover, in this case, the damping ratio was set at 20%, and it was assumed to remain constant and independent of the strain. Of the other layers, relationships between the shear strain, γ; the dynamic shear modulus ratio, G/G_0; and the damping ratio, h, of each layer were set using the estimation formula proposed by Yasuda and Yamaguchi (1985).

The boundary conditions of the analysis model included the side-set energy transfer boundary (vertical fixed, horizontal roller boundary) and the rigid bottom foundation (vertical horizontal fixed). The input seismic wave was based on observation records from the Yumenoshima Observatory of the Bureau of Ports and Harbors, Tokyo Metropolitan Government during the Great East Japan Earthquake. The seismic waves had a maximum acceleration of −61.47 cm/s^2 in the seismic bedrock in earthquake engineering. S-wave velocity of the definition of the seismic bedrock in earthquake engineering is approximately 300 m/s. The inputted acceleration wave performed the amplitude adjusting on the observation record in the ground surface of a nearby site by the one-dimensional seismic response analysis. Therefore, the input seismic wave was used to adjust the value of maximum acceleration at 100 cm/s^2. The time history of input motion is shown in Figure 4.

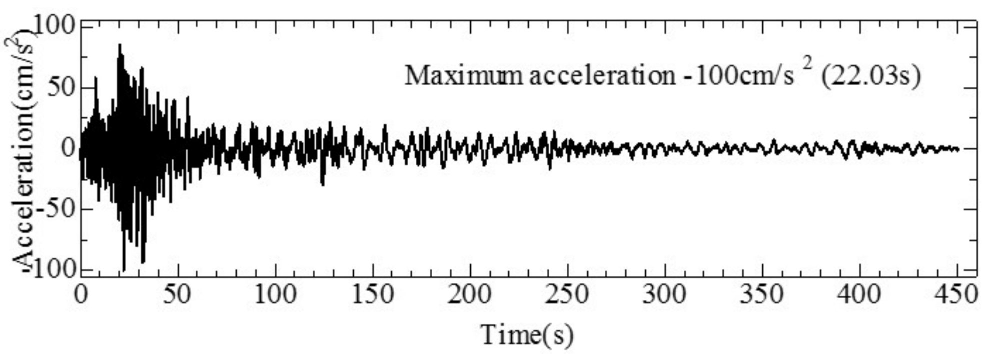

Fig.4 – Time history of input earthquake motion

3.3 Soil properties used in this analysis

The value of soil properties that was used in the analysis was based on physical data that was determined for each layer by the Chiba City (2014). Table 1 shows the list of soil physical properties of the respective layers used in this analysis. The values of γ, D_{50}, ν, and N-value are representative values that were used to perform the soil investigation after the Great East Japan Earthquake in the liquefaction countermeasure promotion in Chiba and were summarized using those results. Shear modulus G (kN/m^2) used in the initial stress analysis was obtained from the following equations:

$$\mathrm{E} = 2800 \times N \tag{1}$$

$$G = \mathrm{E} / \{ 2 \times (1+ \nu) \} \tag{2}$$

Shear modulus at a small strain G_0 (kN/m^2) used in the seismic response analysis was obtained from the following equations:

$$\text{Sandy soil} \quad Vs = 80 \times \mathrm{N}^{\wedge}(1/3) \tag{3}$$

$$\text{Cohesive soil} \quad Vs = 100 \times \mathrm{N}^{\wedge}(1/3) \tag{4}$$

$$G_0 = \gamma / g \times Vs^2 \tag{5}$$

Table 1 – Physical properties of the respective layers used for the analysis

Layer	Soil property	γ (kN/m^3)	D_{50} (mm)	ν	*N*-value	*V*s (m/s)	*E* (kN/m^2)	*G* (kN/m^2)	G_0 (kN/m^2)
B	Sandy soil	17.0	0.150	0.333	10	172	28000	10503	51531
Fsc	Silty sand	17.0	0.150	0.496	5	137	14000	4679	32463
Fs	Silty sand	18.0	0.150	0.493	3	115	8400	2813	24452
Fc-1	Silty	15.0	0.100	0.496	1	100	2800	936	45306
Fc-2	Sandy silt	17.0	0.015	0.497	2	126	5600	1870	27537
Acs	Sandy silt	18.0	0.020	0.492	3	144	8400	2815	38206
As-1	Fine sand	18.5	0.030	0.495	11	175	30800	10301	59757
As-2	Fine sand	18.5	0.150	0.491	12	183	33600	11268	63326
Ac	Sand mixed silt	18.0	0.020	0.492	11	222	30800	10322	90847
Dc	Sand mixed silt	16.0	0.020	0.489	16	252	44800	15044	103667
Ds-1	Fine sand	19.5	0.150	0.476	32	254	89600	30352	128358
Ds-2	Fine sand	19.5	0.150	0.470	50	295	140000	47619	172836

where γ = Unit weight of the soil (kN/m^3), D50 = mean particle diameter of the soil (mm), ν = Poisson's ratio, N = measured SPT N-value

4. Results of seismic response analysis

The results of the analysis were organized the maximum acceleration distribution (Case 1) for the seismic response analysis in each section was obtained.And showed the maximum displacement distribution (Case 4) of conditions that lowered the shear modulus which the sloshing after liquefied. Next, it organized the maximum horizontal directional strain within the ground at each depth. This was done by organizing the tensile and compressive strain points of GL −0.0, −3.0, −5.0, and −7.0 m. It is to examine the occurrence point of the horizontal strain.

4.1 Cross-section 2–2' of the analysis results and discussion

Figure 5 shows the 2–2' cross-sectional analysis model. This cross-section shows the feature that the liquefied layers were greatly inclined in the vicinity of 360 m. From this, the Fsc layer of landfill soil can be seen to thickly deposit towards the sea on the 2' side. In addition, each layer from the Fc2 layer and deeper is almost horizontally deposited.

The maximum acceleration distribution (Fig.6) shows a response of approximately 400 cm/s^2 near the ground surface. In particular, the maximum acceleration increases in the vicinity of 150 and 300 m. Since the fragile Fc1 layer is thickly deposited, it is considered that the acceleration has been amplified. Figure 7 shows the maximum displacement distribution of the sloshing. The maximum displacement increases on the right side of the liquefied layer from 350 m, and there is a maximum of approximately 10 cm.

The discussion continues with the horizontal direction compressive and tensile strains, which are thought to have influenced the buckling damage to the roads by sloshing. Thus, the maximum strain distributions in the horizontal direction, at four selected depths from GL −0.0 m to GL −7.0 m (Fig.5) are shown in Figure 8. From these figures, it can be confirmed that the strain in the Case 1 horizontal direction almost did not occur. By contrast, when the shear stiffness gradually decreased in Cases 4 through 2, a large horizontal direction strain was partially generated. If we look from deeper in the order, it can be confirmed that a horizontal strain in the vicinity of between 300 to 400 m has occurred at the GL −7.0 m point. This depth is considered to be correct because there is a boundary of liquefied and non-liquefied layers such as Fsc and Fc1. In addition, at GL −5.0 m, horizontal strain occurs in the vicinity of 400 to 500 m. This depth is also considered to be correct because there has boundary of liquefied and non-liquefied layers such as Fsc and Fc1. Further horizontal strain occurred elsewhere at GL −3.0 m and GL −0.0 m. From the damage positions on the ground surface plotted in Figure 5, this position indicates a tendency to somewhat match the strain-generating portion. The cause of the ground surface damage, liquefaction in the vicinity of the liquefied layer at lower depths, and the strain that occurred at the boundary of the non-liquefied layer are thought to be caused by overlapping.

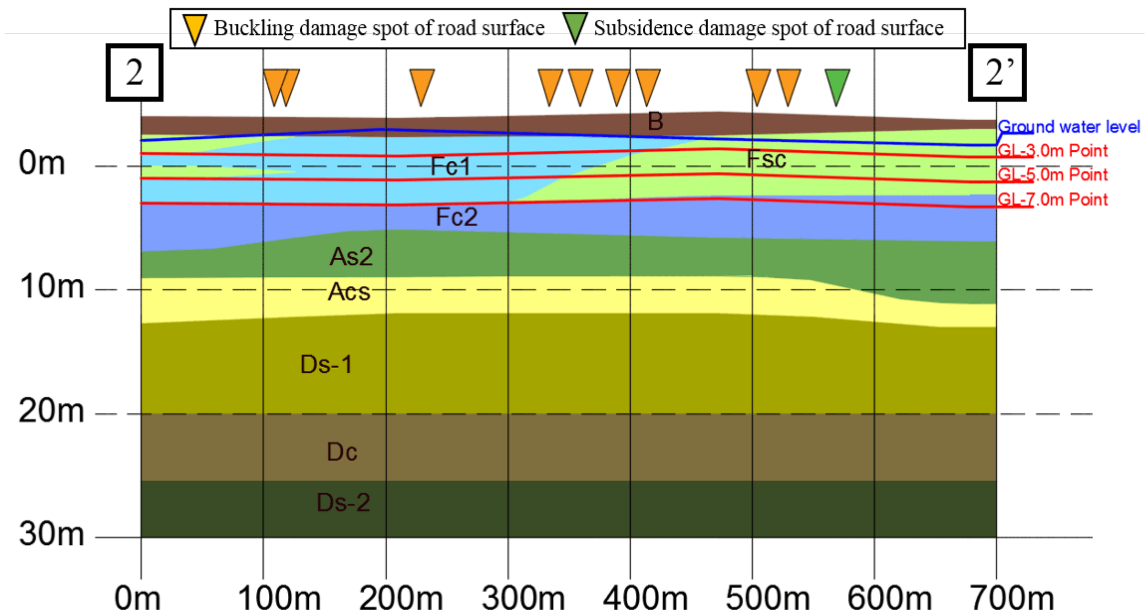

Fig.5 – Survey line 2–2' of the analysis model

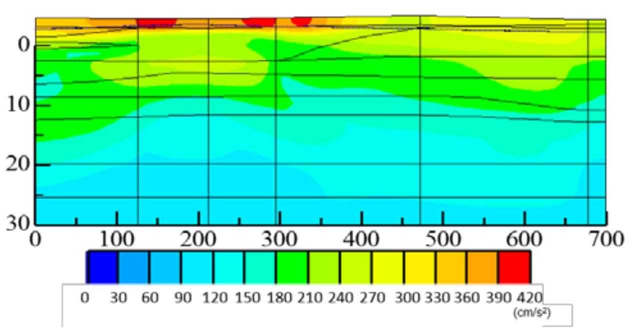

Fig.6 – Cross-section 2–2' maximum acceleration distribution (Case 1)

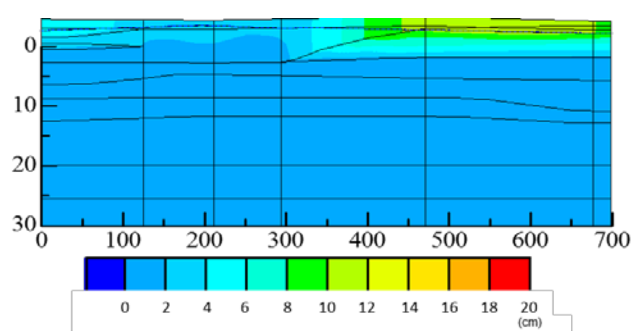

Fig.7 – Cross-section 2–2' maximum displacement distribution (Case 4)

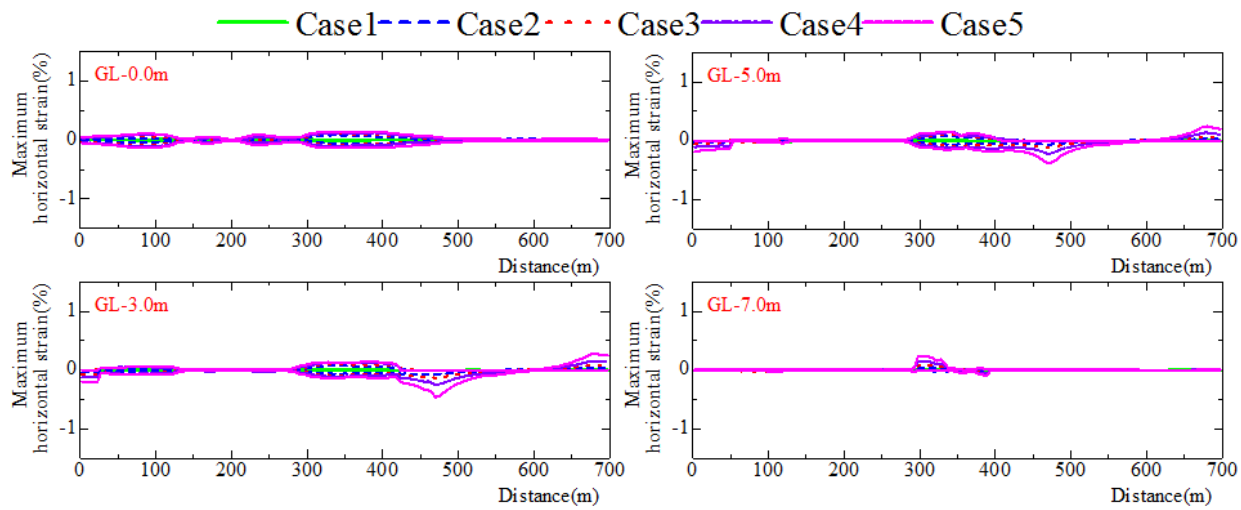

Fig.8 – Cross-section 2–2' maximum horizontal strain distribution for each depth

4.2 Cross section IV–IV' of the analysis results and discussion

Figure 9 shows the IV–IV' cross-sectional analysis model. In this cross-section there is a discontinuous layer boundary within the landfill between 400 to 500 m, and liquefied layer is thickly deposited in the vicinity of 400 m. In particular, the Fc1 and Fc2 layers are thickly deposited at 500 to 700 m, and the inclination of the liquefied layer lower end is seen at around the same distance. Furthermore, the Fs and As1 layers are mixed in this cross-section, a trend that is not seen in other cross-sections.

Figure 10 shows the maximum acceleration distribution. It shows a response of over 300 cm/s^2 at the ground surface. It is thought to be affected by a complex gradient in the ground present in the lower surface of soft cohesive soil and the upper surface of diluvium. Figure 11 shows the maximum displacement distribution of the sloshing. It has been confirmed by large values that liquefaction is thickly deposited on the IV side. The maximum displacement is larger than 14 cm.

Figure 12 shows the maximum horizontal strain distribution at each depth. If we look from deeper in the order, it can be confirmed that horizontal strain in the vicinity of about 400 m has occurred at the GL −7.0 m point. This depth is considered to be correct because there is a boundary of liquefied and non-liquefied layers such as Fsc and Fc2. In addition, at GL −5.0 m, horizontal strain occurs in the vicinity of 1200 m. The GL −3.0 m point shows larger strain values, but GL −0.0 m shows different strain distribution of the other depth. This is thought to be due to the difference in the organization of strain points between the liquefied and non-liquefied layers. It can be confirmed that the horizontal strain becomes larger as it approaches the ground surface.

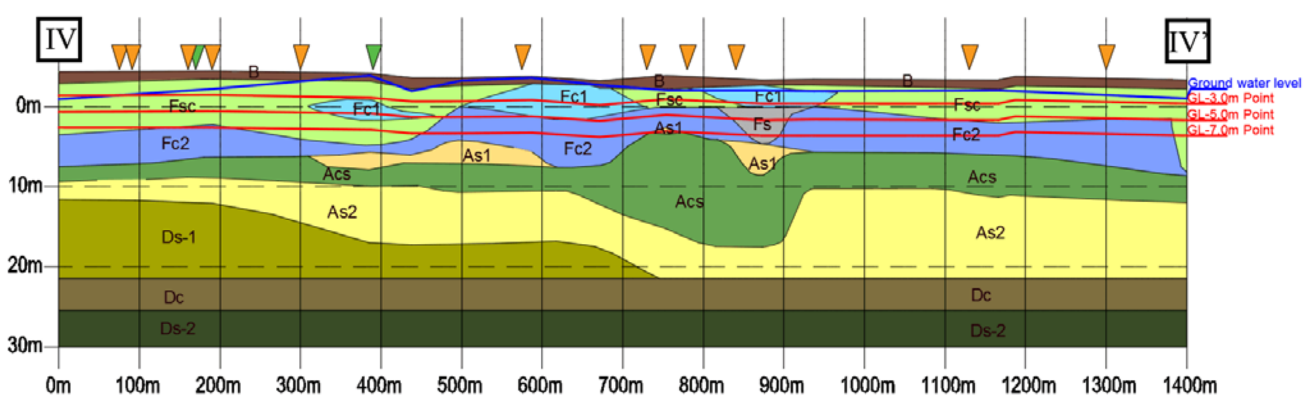

Fig.9 – Survey line IV–IV' of the analysis model

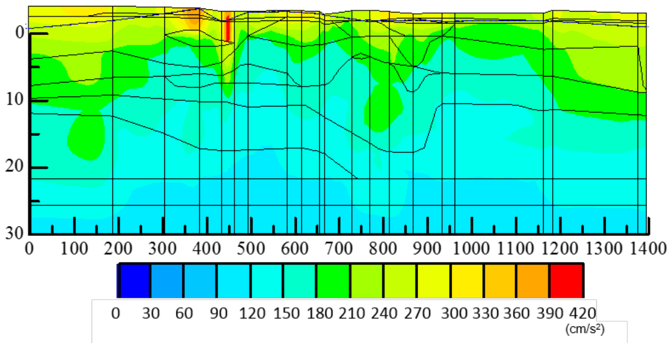

Fig.10 – Cross-section IV–IV' maximum acceleration (Case 1)

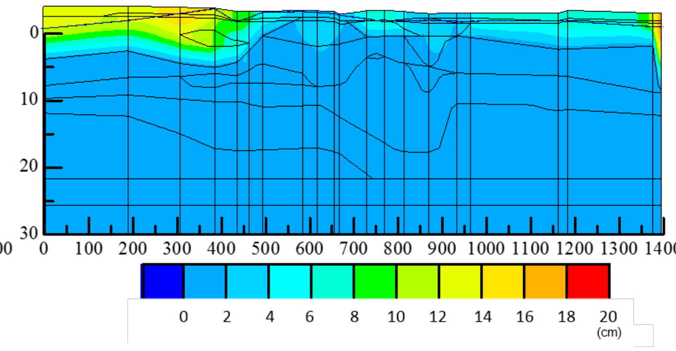

Fig.11 – Cross-section IV–IV' maximum displacement distribution (Case 4)

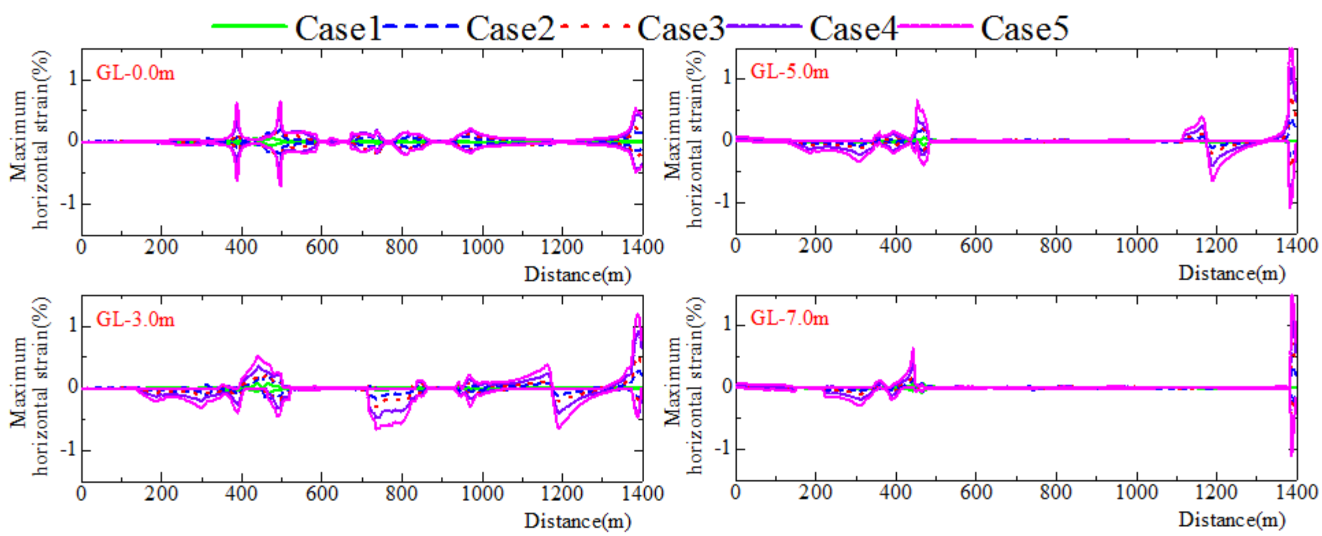

Fig.12 – Cross-section IV–IV' maximum horizontal strain distribution at each depth

4.3 Cross-section V–V' of the analysis results and discussion

Figure 13 shows the V–V' cross-sectional analysis model. In the V side, the liquefied Fsc layer by the Great East Japan Earthquake is thickly deposited. Conversely, in the Fc layer it is assumed that non-liquefaction is thickly deposited on the V' side. The feature of this section is that the boundary of liquefaction layer and the nonliquefaction is present in the vicinity of 600 m.

Figure 14 shows the maximum acceleration distribution. As with other cross-sections, acceleration distribution of 270–330 cm/s^2 is seen near the surface, in particular, more than 360 cm/s^2 at approximately 700 m. By considering the maximum displacement distribution in the sloshing of Figure 15, the displacement becomes particularly large when the liquefied layer is more than 25 cm in the vicinity of the 600 m. Conversely, the displacement becomes small (approximately 5 cm) in the vicinity of the 700 m liquefied layer.

Figure 16 shows the maximum horizontal strain distribution at each depth. If we look from deeper in the order, it can be confirmed that the horizontal strain in the vicinity of 400 to 600 m has occurred at the GL −7.0m point. This depth is considered there has a boundary of liquefied and non-liquefied layers such as Fsc and Fc. In addition, at GL −3.0 m horizontal strain occurs in the vicinity of 850, to 1150 m. These depths are also considered to be correct because there is a boundary of liquefied and non-liquefied layers such as Fsc and Fc. Therefore, the horizontal strain of the GL −0 m point that give effect to the Buckling of the road, It is considered that it is the influence of strain in occurred in the vicinity of the boundary of liquefied and non-liquefied layers.

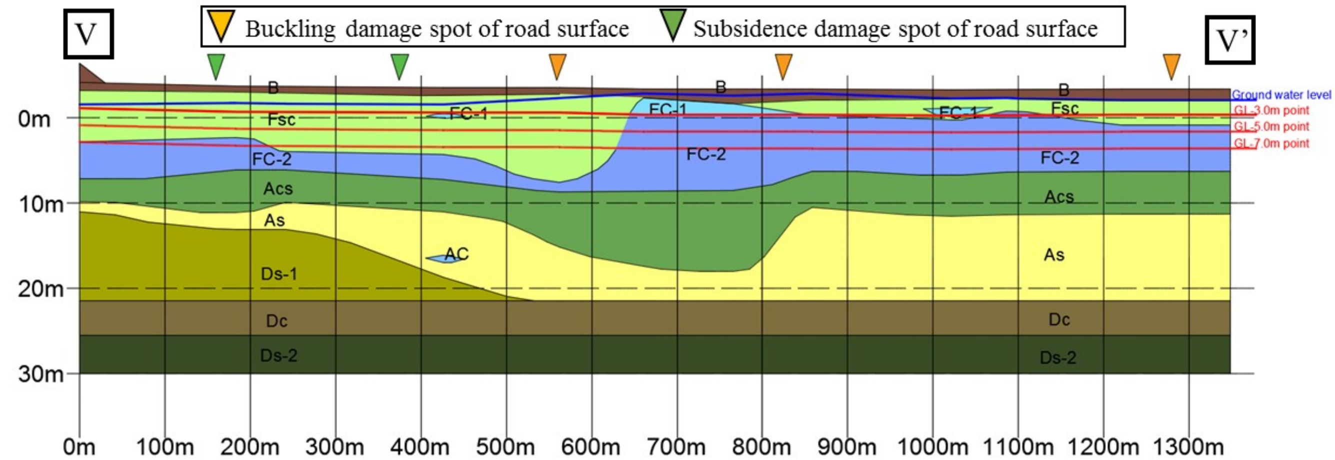

Fig.13 – Survey line V–V' of the analysis model

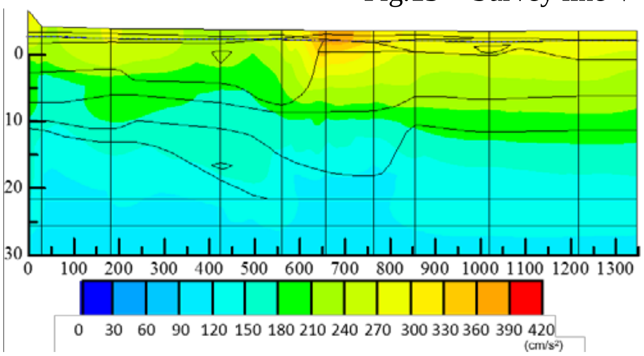

Fig.14 – Cross-section V–V' maximum acceleration (Case 1)

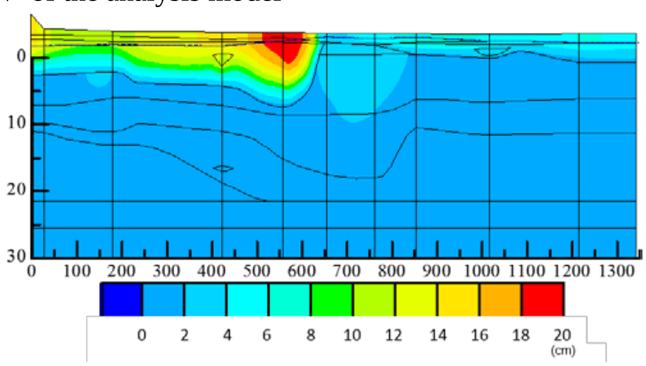

Fig.15 – Cross-section V–V' maximum displacement distribution (Case 4)

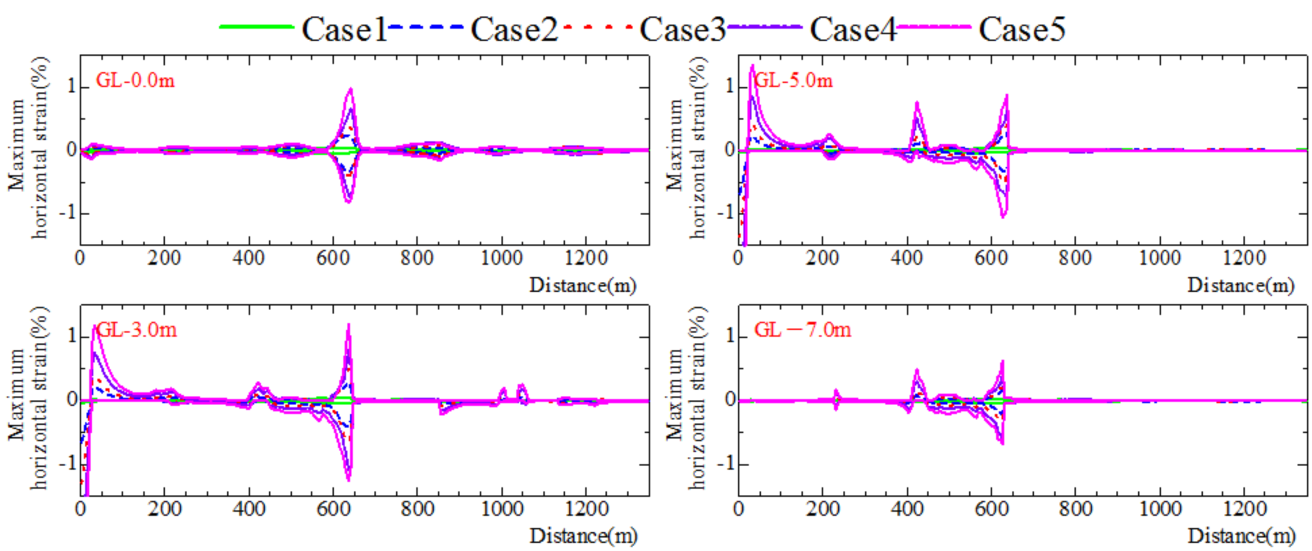

Fig.16 – Cross-section V–V' maximum horizontal strain distribution at each depth

5. Conclusion

The 2011 Great East Japan Earthquake caused significant damage, e.g., the road surfaces underwent buckling damage and the joints of water pipes and gas conduits in the Tokyo Bay area, because a kind of sloshing occurred in the liquefied ground. Two dimensional seismic response analyses were conducted for the soil cross sections where severe damage to roads and buried pipes occurred to demonstrate the mechanism of the sloshing and the damage. The following conclusions were derived through these studies:

(1) Large horizontal strain occurred at the boundary between liquefied layers and non-liquefied layers.

(2) The large horizontal strain amplified from the bottom of the liquefied layers to the ground surface.

(3) Positions where damage to roads and/or buried pipes occurred fairly coincided with the strain-generating portions.

Acknowledgment

This work was supported by JSPS KAKEN Grant Number 26420487.

References

[1] Yasuda S, Ishikawa K, Igarashi S, Tanaka Y, Hatanaka T, Iwase N, Namiki T, Saito N (2014): Study on the Mechanism of the Liquefaction-induced Damage of Water Pipes during the 2011 Great East Japan Earthquake in Urayasu City. *14th Japan Earthquake Engineering Symposium*, Japan. (in Japanese)

[2] Yasuda S, Hagiya S (2012): Thrusting damage of plane road due to liquefaction in Tokyo Bay area. *9th Geotechnical Society Kanto Branch Symposium*, Japan. (in Japanese)

[3] Chiba City (2014): Report of Technical Committee on Urban Liquefaction Countermeasure Project, Japan. (in Japanese)

[4] Tokyo Port Authority HP: For ground motion observed by the Port Authority earthquake observatory. (in Japanese)

[5] Yasuda S, Yamaguchi I (1985): Dynamic deformation properties in a variety of undisturbed soil, *20th geotechnical research recital Proceedings*, 539-542, Japan. (in Japanese)